

2

3 **Physico-Chemical and Mechanical Behavior of**

4 **Natural Clay as a Porous Medium during**

5 **Convective Drying**

6

7 **Saber Chemkhi**

8

9 *Chemical Engineering Department, King Khaled University, Po. Box 394, Abha, KSA.*

10

11 *& Laboratory of Energetic and Thermal Processes, CRTEn, Borj Cedria, BP. 95, Hammam-*

12 *Lif 2050, Tunisia.*

13 **Saber Chemkhi**

14 [\*saberchemkhi@yahoo.fr\*](mailto:saberchemkhi@yahoo.fr)

---

15

16

17

18

19 **ABSTRACT**

20

The present work consists on an experimental characterization of non-purified clay material. The survey is focused on the chemical, physical, and mechanical properties variation during the convective drying of the material. Clay identification by atomic absorption spectrophotometer and X-ray diffractometer are used to determine the exact composition. The study covers also essential physical properties of the material such as density, volume shrinkage, and porosity in one hand, and the mechanical properties: Young modulus and the parameters of viscoelastic behavior for the other hand. The novelty is the variation of the properties function of the material moisture content. The clay was identified kaolinite as major fraction. The true density is evaluated to (2685 +/- 35 kg/m<sup>3</sup>). And Young modulus is about (15 MPa) for dried material. The results are judged to be acceptable comparing to the literature data.

21

22 *Keywords: Non-purified clay; atomic absorption spectrophotometer; X-ray diffractometer;*

23 *Convective drying; Density; Volume shrinkage; Porosity; Young modulus; Viscoelasticity.*

24

25

26 **1. INTRODUCTION**

27

28 Clay is a raw material used in construction materials like cement, bricks, and ceramics. In

29 Tunisia, this industry is one of the most important sectors in the national economy and it

30 consumes huge amounts of energy. In 2011, it is estimated to 827.5 kTEP (57.4% of the

31 national energy consumption in the industry sector). And especially, the drying process

32 consumes 96.7 kTEP (6.7% of the national energy consumption in the industry sector) [1].

33 Clay is also considered as the typical inorganic raw material used for ceramic products,

34 which are commonly manufactured using traditional methods. The demand for ceramics is

35 increasing in several diverse fields. The application ranges from materials for house ware

36 and buildings to highly functional materials called "fine ceramics". Drying is one of the

37 important steps of ceramics manufacturing [2, 3]. And the modeling of drying is important to  
38 foresee the quality of the final product.

39 Clay brick masonry is one of the oldest and most durable construction techniques used by  
40 mankind. The manufacture of fired clay bricks can be divided generally into four stages.  
41 Firstly, the extraction and the storage of the raw material. After storage, clay is crushed and  
42 mixed with water. The resulting mix is characterized by enough plasticity to facilitate the  
43 molding. The crude clay is then dried by different processes. Generally, the drying process  
44 takes a lot of time and can still for one week or more. Finally, the hardening of the bricks in  
45 order to acquire additional resistance. The material is fired in a kiln with high temperature  
46 (more than 1000°C).

47 Drying is an important process step in the bricks manufacturing [3]. The drying related  
48 problems are cracks and deformations that may take place due to the volume shrinkage.  
49 Drying is usually carried out slowly, although fast drying cycles are widely industrially  
50 practiced.

51 The originality of this work is that it deals with non purified clay. In literature, most of works  
52 are done on purified clays such as kaolinite [4, 5] and bentonite [6]. The aim of this work is to  
53 characterize our product to collect data for the sector of bricks and ceramics manufacturing.

54

## 55 2. MATERIAL AND METHODS

56

### 57 2.1 Clay identification and characterization

58 Natural clay extracted from “*Tabarka*” region in Tunisia was used as a model material in this  
59 study. The characterization was done by atomic absorption spectrophotometer (type Perkin  
60 Elmer 560) [2, 7], major elements contents being determined. Also, loss in ignition at 1000°C  
61 was obtained. X-ray diffractometry allowed identify the main clay mineral components [2, 7].

62

### 63 2.2 Clay drying

64 The drying experiments were carried out in a convective drying tunnel (see Fig. 1) with wet  
65 air whose parameters (temperature, velocity, and humidity) are controlled and regulated.  
66 The clay samples are molded in a plate form with dimensions of (15\*12\*1.5 cm). The mass  
67 evolution during drying is taken with an electronic precision balance, then stored using an  
68 acquisition program.

69 The accuracy of the measurement is as follows: (0.001 g) for the mass, (0.1°C) for  
70 temperature, (0.1 m/s) for the air velocity, and (1%) for the relative humidity.

71



72

73 **Fig. 1 Experimental setup for the convective dryer**

74  
75 The experimental conditions for the clay drying are presented in the table 1. Temperature  
76 variation between (40 and 60°C), and relative humidity range (30-60%). The air velocity is  
77 fixed at (2 m/s). Initial moisture content of the clay samples is about (0.2 +/- 0.003 kg/kg dry  
78 mass).

79  
80 **Table 1. Experimental conditions for the convective clay drying.**

| <b>Experiments</b> | <b>Temperature (°C)</b> | <b>Air velocity (m/s)</b> | <b>Relative humidity (%)</b> | <b>Initial moisture content (kg/kg)</b> |
|--------------------|-------------------------|---------------------------|------------------------------|---|
| 1                  | 50                      | 2                         | 30                           | 0.203                                   |
| 2                  | 50                      | 2                         | 40                           | 0.200                                   |
| 3                  | 50                      | 2                         | 60                           | 0.204                                   |
| 4                  | 40                      | 2                         | 40                           | 0.198                                   |
| 5                  | 60                      | 2                         | 40                           | 0.202                                   |

81  
82 The drying curves can be modeled using some mathematical equations presented in table 2,  
83 to be fitted and to find the best model describing the drying kinetics.

84  
85 **Table 2. Mathematical models of the drying curves [8]**

| <b>Model Name</b>                           | <b>Equation of the model</b>   |
|---|--------------------------------|
| <i>Wang and Singh</i>                       | $MR = 1 + a.t + b.t^2$         |
| <i>Multiple Multiplicative Factor Model</i> | $MR = (a.b + c.t^d)/(b + t^d)$ |
| <i>Henderson and Pabis</i>                  | $MR = a.exp(-kt)$              |
| <i>Logarithmic</i>                          | $MR = a.exp(-kt) + b$          |
| <i>Midilli equation</i>                     | $MR = a.exp(-k(t^d) + b.t$     |

86  
87 Regression analyses of these equations were done by using regression models. The  
88 performance of the different models was evaluated using various statistical parameters such  
89 as the regression coefficient (r) and the standard error (S). These parameters can be  
90 calculated as following:

$$S = \sqrt{\frac{\sum_{i=1}^{n_{points}} (y_i - f(x_i))^2}{n_{points} - n_{param}}} \quad (1)$$

$$r = \sqrt{\frac{S_t - S_r}{S_t}} \quad (2)$$

$$S_t = \sqrt{\sum_{i=1}^{n_{points}} (\bar{y} - y_i)^2} \quad (3)$$

$$S_r = \sum_{i=1}^{n_{points}} (y_i - y(x_i))^2 \quad (4)$$

$$\bar{y} = \frac{1}{n_{points}} \sum_{i=1}^{n_{points}} y_i \quad (5)$$

95  
96  
97 **2.3 Physical Properties**

98 Cubic humid clay samples were molded from clay powder mixed with distilled water at a  
 99 moisture content of (0.2 kg/kg). These homogeneous samples of (1 cm<sup>3</sup>) approximate  
 100 dimension were used to determine the evolution of the density with the moisture content.  
 101 They are placed in the convective dryer to reduce their humidity. Every five minutes, one  
 102 sample is taken from the dryer to measure its apparent density. The experiment consists on  
 103 the measurement of the sample weight in air and the corresponding buoyancy force in  
 104 methanol. On the figure 2, is given a photo of the experimental apparatus mounted on a  
 105 precision balance.  
 106 The corresponding moisture content of the sample is determined by the measure of the ratio  
 107 of humid and dry masses. All samples are placed in an oven at (105°C) during (24 hours) to  
 108 eliminate all the humidity.  
 109 The true density of the solid (intrinsic density) is determined by pycnometry. A standard (50  
 110 mL) pycnometer was used in this stage. The measurements were performed in triplicate  
 111 and we take the mean value.  
 112



113 **Fig.2. Experimental apparatus for the apparent density determination installed with a**  
 114 **precision balance.**  
 115  
 116

117 **2.3.1 Apparent density**

118 As it is mentioned above, the apparent density is determined by measurement of the sample  
 119 weight in air and the corresponding buoyancy force in methanol. The following equation  
 120 (correspond to the apparatus) is used to calculate the density of all samples.  
 121 Apparent density ( $\rho$ ) was determined with the principle of Archimedes. This property is  
 122 calculated by using the following correlation related to the used experimental apparatus:

123 
$$\rho = \frac{M_a(\rho_f - 0,0012)}{0,99983 * G} + 0,0012 \quad (6)$$

124 With  $\rho$  is the apparent density,  $\rho_f$  is the fluid (methanol) density,  $M_a$  is the solid mass in air,  
 125 and  $G$  is the hydrostatic buoyancy.  
 126

127 **2.3.2 Volume shrinkage**

128 The volume shrinkage is determined indirectly by the density measurement. There is a  
 129 relation between specific volume and density:

130 
$$R_v = \frac{V(X)}{V_0} = \frac{\rho_0(1+X)}{\rho(1+X_0)} \quad (7)$$

131

132 **2.3.3 Porosity**

133 To calculate the gas porosity of the presented formulation uses, through Eq. 8, the following  
134 properties of the medium: initial moisture content, initial density and true density [9].

135 
$$\Phi_g = \frac{Z - (1 - \Phi_0)Y}{Z} \quad (8)$$

136 Note that **Z** is the experimental shrinkage, **Y** is the ideal shrinkage (Eq. 9),  $\Phi_0$  is the initial  
137 porosity of the medium (Eq. 10) and  $\beta$  is the ratio of the solid true density and the liquid one  
138 (Eq. 11).

139 
$$Y = \frac{\rho_0}{1 + X_0} \left( \frac{1}{\rho_s^s} + \frac{1}{\rho_l^l} \right) \quad (9)$$

140 
$$\Phi_0 = 1 - \frac{\rho_0(1 + \beta X_0)}{\rho_s^s(1 + X_0)} \quad (10)$$

141 
$$\beta = \frac{\rho_s^s}{\rho_l^l} \quad (11)$$

142

143 **2.4 Mechanical Properties**

144 This experimental work is introduced in order to approach the phenomena of elasticity and  
145 viscoelasticity attributed to the clay material. Many experiments were carried out to identify  
146 the parameters related to the viscoelasticity and deepen the knowledge of the structure of  
147 clays (Natural clay extracted from "Tabarka" region in Tunisia was used as a model  
148 material in this study).

149

150 **2.4.1 Compression test: Methodology**

151 The compression test is done to evaluate the Young Modulus of the material. Fine-grained  
152 unpurified clay powder was saturated with distilled water to produce slurry. This mixture  
153 of (30%) water content was subsequently thoroughly stirred to ensure complete  
154 homogenization of the slurry. The material is molded in cylindrical shape (27 mm diameter  
155 and 10 mm height).

156 Samples were tested using a traction-compression machine (LRX Plus) with console (Ref.  
157 No. 01/2962) shown in Figure 3. It served to determine the modulus of elasticity (Young's  
158 modulus) of the clay with a test speed equal to (0.1 mm/min).

159



160

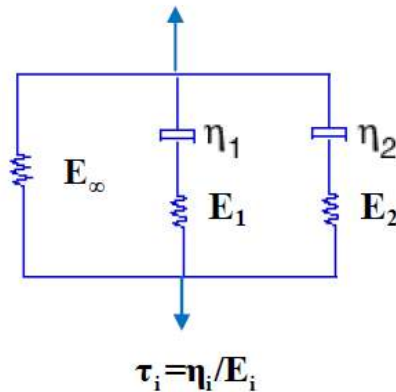
161 **Fig.3. Traction compression machine (LRX Plus) with console (Ref. No. 01/2962).**

162

163 **2.4.2 Parameters of the viscoelastic behavior**

164 The viscoelastic nature of the clay can be studied by examining the temporal evolution of the  
165 clay's response following a set of tests such as the relaxation, the creep or oscillating  
166 stresses. Since the clay is considered as a solid and remains until the end of the drying, the  
167 Kelvin Voigt model is the best choice to describe its behavior [10-11].

168 The viscoelastic behavior can be presented using rheological models using springs (elastic  
 169 character) and dashpots (viscous character) linked in series or in parallels.  
 170



171  
 172 **Fig.4. Simplified rheological model for clay [13].**  
 173

174 The experimental study conducted for the rheological characterization of the clay is derived  
 175 from an application of a constant strain using the same traction-compression machine.  
 176 Depending on water content, the results show that the relaxation level of equilibrium is  
 177 reached for times greater than 10 hours. Relaxation time is higher for the more sample is  
 178 dried. The viscosity significantly decreases within water content. In fact, the liquid phase  
 179 escape is used to relax the solid matrix. According to works in the rheology field which have  
 180 shown that the delay time (after creep) is higher than relaxation time [12], the values of the  
 181 relaxation time experimentally quantified were considered for the move to increase with  
 182 delay time (result of creep test).

183  
 184 **3. RESULTS AND DISCUSSION**

185  
 186 **3.1 Clay characterization**

187 If we examine table 3, we can conclude that the major fraction of the clay is silica. It is also  
 188 rich in Iron, Aluminium, and Potassium. The other compounds are less than 2.5 %. The  
 189 losses in ignition are also important due the nature of clay (natural: non purified).  
 190 The results of the X-ray diffractometer are presented in figure 5. From the figure above, it is  
 191 clear that the major fraction of the crystalline phase is quartz and kaolinite.

192  
 193 **Table 3. Chemical composition of clay in mass percentage.**

| <i>Oxides</i> | <i>SiO<sub>2</sub></i> | <i>K<sub>2</sub>O</i> | <i>Al<sub>2</sub>O<sub>3</sub></i> | <i>Fe<sub>2</sub>O<sub>3</sub></i> | <i>Na<sub>2</sub>O</i> | <i>CaO</i> | <i>MgO</i> | <i>MnO</i> | <i>L. I.</i> |
|---------------|------------------------|-----------------------|------------------------------------|------------------------------------|------------------------|------------|------------|------------|--------------|
| <i>Mass %</i> | 39.4                   | 15.61                 | 13.85                              | 14.1                               | 0.68                   | 1.14       | 0.56       | 0.13       | 14.44        |

194

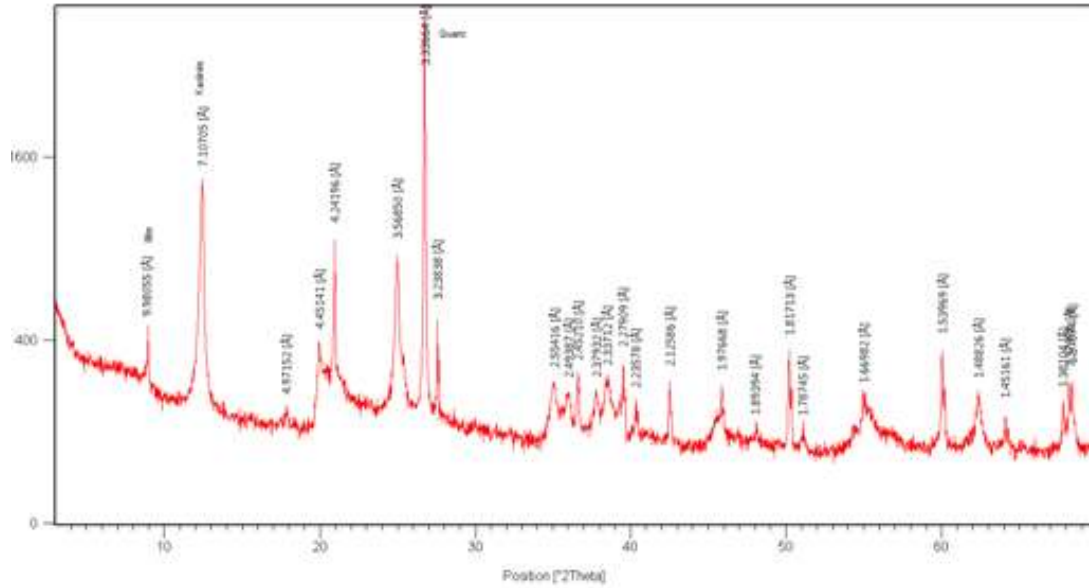


Fig. 5. X-ray diffraction pattern for clay

195  
196  
197  
198  
199  
200  
201

### 3.2. Drying Kinetics

The results of the convective drying kinetics of clay at the different experimental conditions are presented in Figure 6. The total drying time is about 22 hours.

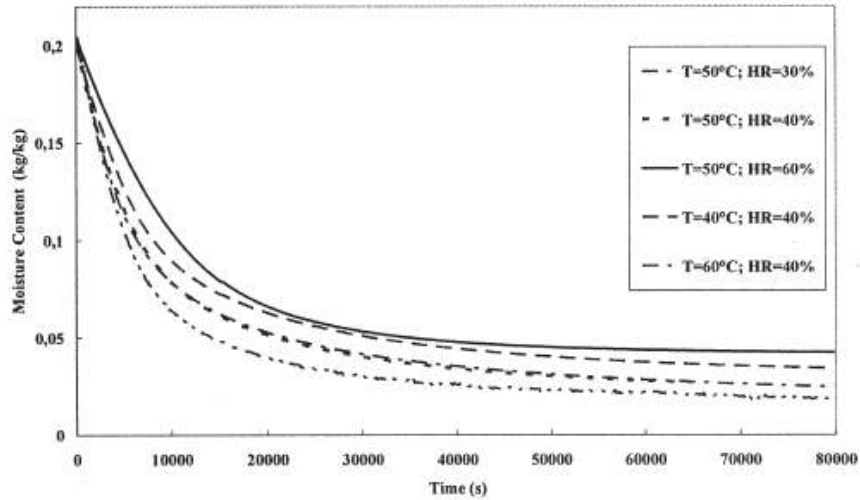


Fig. 6. Drying of clay at different conditions

202  
203  
204  
205  
206  
207  
208  
209  
210  
211

### 3.3. Density, Volume shrinkage, and Porosity

The results of the density variation with the moisture content are presented on the figure 7. For the true density of the clay was evaluated as (2685 +/- 35 kg/m<sup>3</sup>).

The volume shrinkage is plotted in Fig.8. It reflects a good prediction of this parameter. The difference is within the pattern established for the (2D) simulation model contrary to the nature of this parameter (3D).

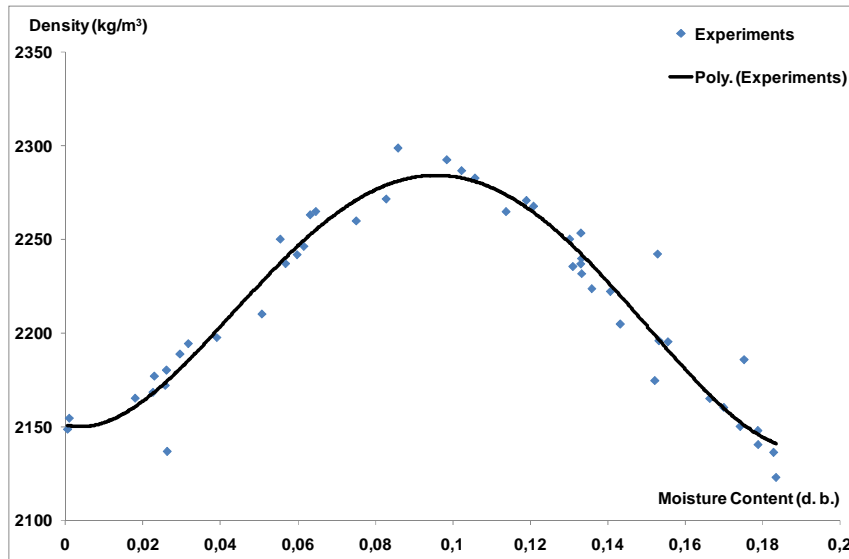


Fig. 7. Clay density versus moisture content.

212  
213  
214

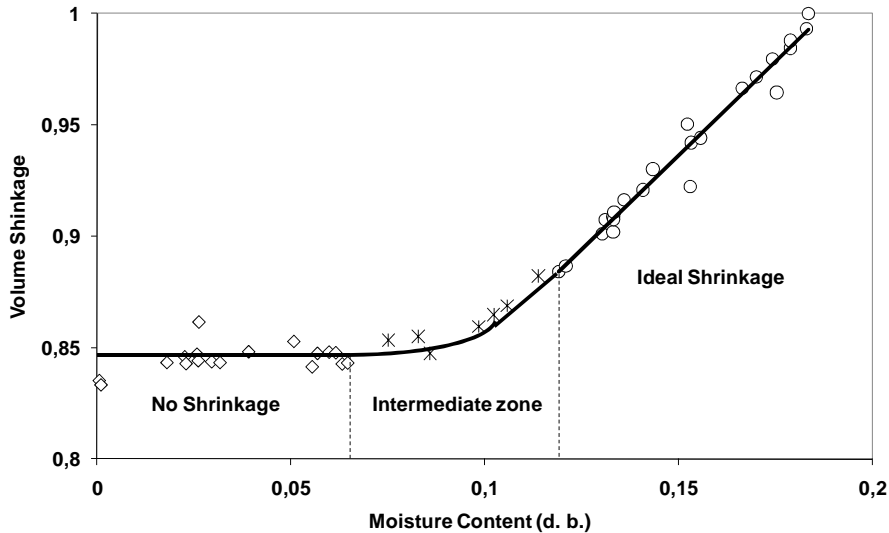


Fig. 8. Volume shrinkage versus moisture content

215  
216  
217

As it is still a validation of a model proposed by referring to the experimental study, the constants used for this study are:

- 220  $\rho_0=2123 \text{ kg/m}^3$
- 221  $\rho_s^s=2685 \text{ kg/m}^3$
- 222  $\rho_l=1000 \text{ kg/m}^3$
- 223  $X_0=0.1835 \text{ kg/kg}$ .

224 From Fig.8, the water content decreases highlighting a gap in the structure of the material  
225 filled with a volume shrinkage increasing to register a water content using the presence of a  
226 third phase other than the solid and liquid. The gas begins to be in the material pores. Figure  
227 9 shows that this phase is negligible up to water content nearly equal to 0.086 (saturated  
228 medium). Then, the medium becomes unsaturated and the air porosity increases quickly to  
229 20% for dry material.

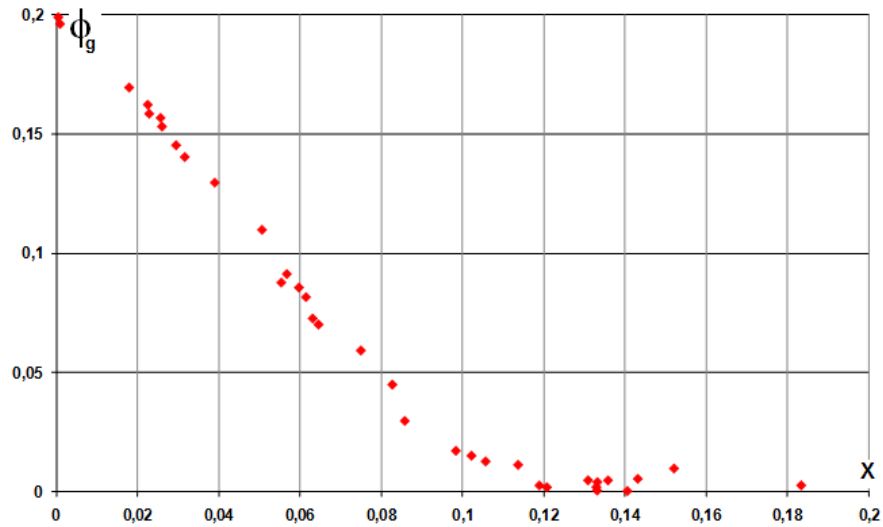


Fig.9. Porosity gaseous ratio versus moisture content.

231

232

233

234

### 3.4. Young modulus and viscoelastic parameters

235

236

237

238

239

240

241

242

243

244

245

246

247

248

249

250

251

252

253

254

255

256

257

258

259

260

261

262

263

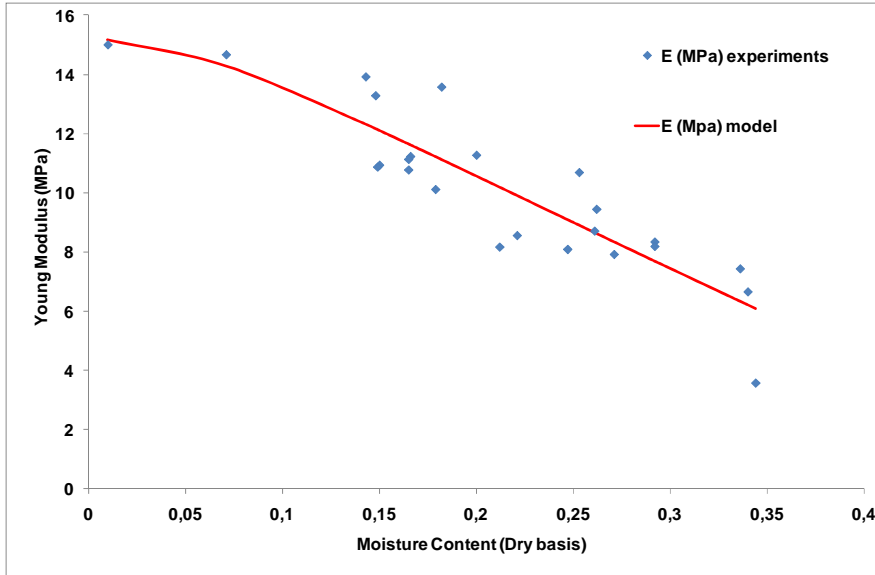
264

The response of the material to compression is a function of the water content. This result matches with those obtained in the literature [14]. For a range of water contents close to 15%, the clay behaves pure elastic. For water contents close to 30%, the material behaves like a non-linear elastic medium. For water contents below 10%, the clay is similar to the behavior of brittle materials: the stress tends to increase much in the deformation range of elastic domain. Note that the drop in stresses corresponds to visible cracks on the sample tested faces.

Unlike what is common to the relations linearity to determine the Young modulus, the evolution of stresses-strains depends on what is small or large deformations hypothesis. To distinguish different modulus of elasticity, we adopt the following citation [15]: "In the first zone, designated as elastic, the modulus reaches a value almost independent of the level of distortion. Deformations are very small in this area. Therefore the modulus is generally described as 'maximum' or 'initial' ( $E_{max}$ ). In the following areas, the modulus decreases with increasing deformations. Monotonic curves are described by a 'secant' modulus ( $E_{sec}$ ) defined by the slope of the line connecting the origin to the current module. And a tangent one ( $E_{tan}$ ) determined by the slope of the curve in neighborhood of the point".

Al Husein [16] introduced, as well, the difficulty of choosing the deformations modules. In referring to his thesis (soils and geotechnical): "it's often advisable to take a medium modulus, for example the one corresponding to a level equal to 50% of diverter at break".

The question that arose at this stage of the study was the level of strains to be considered always to ensure a result on the elastic domain. In the case of Mrani work [17], the agar gel's elasticity modulus is calculated from the average slope of the lines for loading and unloading. Characterization of this modulus, in the work of Pourcel [18] on the alumina gel, was based on calculating the slope between 1 and 3% strains. Kowalski et al., [14] worked on the kaolin's elastic modulus by determining this characteristic in a strain equal to 0.2%. The choice of Collard [19] regarding the line slope of 0 to 1% strain was chosen in our work. Note that Collard used plates of clay of the same composition as ours, as reference material. We chose to present the secant Young Modulus versus moisture content in figure 10. The curve presented is the result of the fitting model.



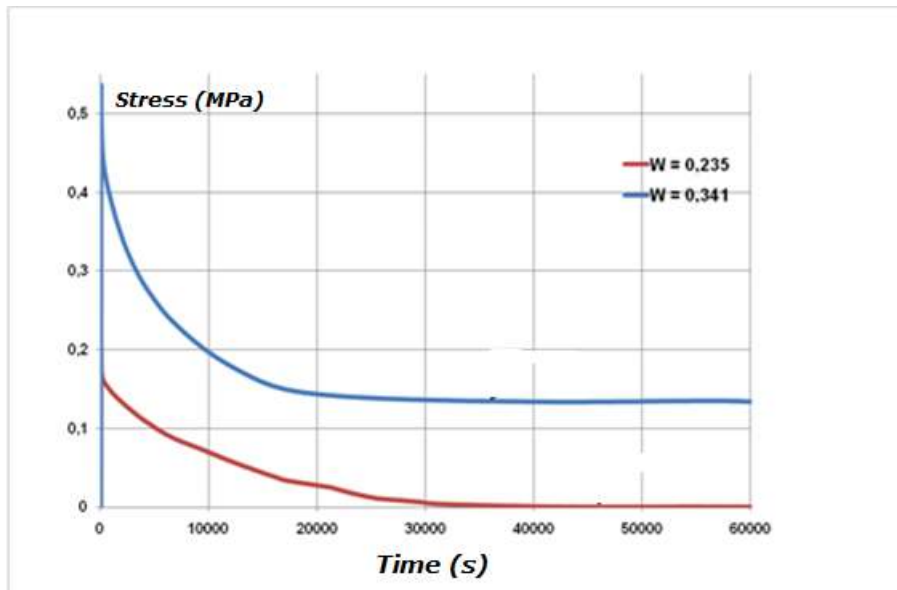
265  
266 **Fig. 10. Evolution of the secant Young modulus of the clay versus water content.**  
267

268 This evolution can be presented by the following relation between Young modulus and  
269 moisture content:

270 
$$E(X) = a - b \exp(-cX^{-d}) \quad (12)$$

271 With the constants:  $a=15.187$ ;  $b=423.83$ ;  $c=2.79$ ; and  $d=0.3$ .

272  
273 The experimental relaxation tests are done using many samples of the product at different  
274 moisture content. Two curves are presented in Fig. 11.  
275



276  
277 **Fig. 11. Relaxation function curves for two moisture contents.**  
278

279 The fitted results of the experimental data for relaxation function using a Prony series gives:

280 
$$E(t) = E_0 + E_1 \exp(-t/\tau_1) + E_2 \exp(-t/\tau_2) \quad (13)$$

281 With the constants:  $E_0=0.018$  MPa;  $E_1=0.21$  MPa;  $E_2=0.66$  MPa;  $\tau_1=40$  s; and  $\tau_2=4500$  s.

282  
283  
284  
285  
286  
287  
288  
289  
290  
291  
292  
293  
294  
295  
296  
297  
298  
299  
300  
301  
302  
303  
304  
305  
306  
307  
308  
309  
310  
311  
312  
313  
314  
315  
316  
317  
318  
319  
320  
321  
322  
323  
324  
325  
326  
327  
328  
329  
330  
331  
332  
333  
334

#### 4. CONCLUSIONS

This paper presents some essential properties of natural clay material to understand its behavior during the convective drying process. Clay identification by atomic absorption spectrophotometer and X-ray diffractometry was shown quartz and kaolinite as major fractions. The main results of this study are: clay density, volume shrinkage and porosity are determined versus its moisture content. The true density was evaluated as (2685 +/- 35 kg/m<sup>3</sup>). Young modulus decreases with moisture content and it is about (15 MPa) for the dried material. The viscoelastic behavior of the material is underlined via the relaxation function determined experimentally. All these results can be useful for the modeling and simulation of the drying process of clay made products.

#### COMPETING INTERESTS

Author has declared that no competing interests exist.

#### AUTHORS' CONTRIBUTIONS

The author read and approved the final manuscript.

#### REFERENCES

1. Agence Nationale des Energies Renouvelables, *Energy Audit Report*, Tunisia, 2011.
2. Chemkhi, S., Zagrouba, F., Bellagi, A. Drying of ceramics: modelling of the thermo-hydro elastic behavior and experiments, *Industrial Ceramics*. 2005: 25 (3): 149-156.
3. Gong, Z.X., Mujumdar, A.S., Itaya, Y., Mori, S., Hasatani, M. Drying of clay and nonclay media: heat and mass transfer and quality aspects, *Drying Technology*, 1998: 16 (6): 1119-1156.
4. Chemkhi, S., Zagrouba, F., Bellagi, A. Thermodynamics of water sorption in clay, *Desalination*. 2004: 166, 393-399.
5. Chemkhi, S., Zagrouba, F. Development of Darcy-flow model applied to simulate the drying of shrinking media, *Brazilian Journal of Chemical Engineering*. 2008: 25 (3): 503-514.
6. Mihoubi, D., Bellagi, A. Thermodynamic analysis of sorption isotherms of bentonite, *Journal of Chemical Thermodynamics*. 2006: 38: 1105-1110.
7. Usman, M.A., Ekwueme, V. I., Alaje, T. O., Mohammed, A. O. Characterization, acid activation, and bleaching performance of Ibeshe clay, Lagos, Nigeria. *ISRN Ceramics*. Volume 2012: Article ID 658508: 5 p.
8. Kemp, I.C., Fyhr, B. C., Laurent, S., Roques, M.A., Groenewold, C.E., Tsotsas, E., Sereno, A.A., Bonazzi, C.B., Bimbenet, J.J., Kind, M. Methods for processing experimental drying kinetics data, *Drying Technology*. 2001: 19 (1): 15-34.
9. Madiouli, J., Lecomte, D., Nganya, T., Chavez, S., Sghaier, J., and Sammouda, H. A Method for determination of porosity change from shrinkage curves of deformable materials, *Drying Technology*. 2007: 25 (4): 621-628.
10. Hasatani M., Itaya Y., Hayakawa K. Fundamental study on shrinkage of formed clay during drying: viscoelastic strain-stress and heat moisture transfer, *Drying Technology*. 1992: 10 (4): 1013-1036.
11. Bulicek, M., Malek, J., Rajagopal, K.R. On Kelvin-Voigt model and its generalizations, Research team 1. Center for Mathematical Modeling, Mathematical Institute of the Charles University, Sokolovska, 2010: 1-8.
12. Witasse, R., Georgin, J.F., Reynouard, J.M., Berthollet, A., Dauffer, D., Chauvel, D. Contribution for modelling creep and drying shrinkage of reinforced concrete structures, *Structures and Materials*. 2000: 6: 577-586.

- 335 13. Hammouda, I., Mihoubi, D., Modelling of drying induced stress of clay: elastic and  
336 viscoelastic behaviours. *Mechanical Time-dependent Materials*. 2014: 18(1), 97-111.
- 337 14. Kowalski, S.J., Banaszak, J., Rybicki, A. Plasticity in materials exposed to drying.  
338 *Chemical Engineering Science*. 2010: 65: 5105-5116.
- 339 15. Nguyen Pham, P.T. Étude en place et au laboratoire du comportement en petites  
340 déformations des sols argileux naturels. Ph.D. Thesis, École Nationale des Ponts et  
341 Chaussées, France, 2008.
- 342 16. Al Husein, M. Étude du comportement différé des sols et ouvrages géotechniques.  
343 Ph.D. Thesis, University of Aleppo, Syria, 2001.
- 344 17. Mrani, I., Bénet, J.C., Fras, G., Zrikem, Z. Two dimensional simulation of  
345 dehydration of a highly deformable gel: Moisture content, stress and strain fields.  
346 *Drying Technology*. 1997: 15 (9): 2165-2193.
- 347 18. Pourcel, F., Jomaa, W., Puiggali, J. R., Rouleau, L. Crack Appearance during Drying  
348 of an Alumina Gel: Thermo-Hydro-Mechanical Properties. *Drying Technology*, 2007:  
349 25 (5): 759-766.
- 350 19. Collard, J.M., Arnaud, G., Fohr, J.P. The drying-induced deformations of a clay  
351 plate. *International Journal of Heat and Mass Transfer*, 1992: 35 (5): 1103-1114.